Biogeotechnics 4 (2026) 100196

Contents lists available at ScienceDirect

Biogeotechnics

journal homepage: www.keaipublishing.com/en/journals/biogeotechnics/

Experimental study on permeability characteristic evolution for modified silty sand by EICP technology considering influence of dry density

Lei Shi, Huan Zhang, Jiaming Fang, Xiangchun Xu, Jianwei Zhang*

School of Civil Engineering and Architecture, Henan University, Kaifeng 475000, China

ARTICLE INFO

Keywords:
Silty sand
Enzyme-induced carbonate precipitation (EICP)
Dry density
Saturated hydraulic conductivity
Pore characteristic

ABSTRACT

This study investigated the influence of initial dry density to the permeability reduction effect and process for the EICP-treated silty sand. The variation of saturated hydraulic conductivity (K_{sat}) and induced $CaCO_3$ (C_{CaCO_3}) under different initial dry density was used to reflect the treatment effect variation. The relationship between the above two parameters was also investigated under different initial dry density. The pore characteristic, which was reflected by area distribution, size distribution and orientation distribution, was used to give some guidance to analysis the permeability reduction mechanism by EICP technology under different dry density. Some meaningful findings could be obtained through the series of experiments. Firstly, the value of K_{sat} after the treatment would have a decrease and then increase trend with the increase of dry density. The value of C_{CaCO_3} would both have an increase and then decrease trend. The extremum value of K_{sat} and C_{CaCO_3} would both merge in the dry density of 1.55 g/cm^3. Secondly, the quantified analysis for SEM result indicated that the total pore area would have a near linear decrease trend with dry density both before and after the treatment. And the decrease of macropore would be the main reason for decrease of total pore area. Thirdly, a generalized mechanism for permeability reduction influenced by dry density was proposed. The generalized variation mechanism could be described by three aspects, including seepage characteristic, process of $CaCO_3$ attachment and pore orientation distribution variation. We analyzed the process of permeability reduction based on seepage characteristics and focused on the influence of dry density factors on soil permeability changes in EICP treatment, which is crucial for the application of soil treatment.

1. Introduction

The enzyme-induced carbonate precipitation (EICP) is a promising bio-geotechnical technology (Xu et al., 2023; Shu et al., 2022). The EICP technology uses the urease to promote the urea hydrolysis to generate the free CO_3^{2-}, which would react with the Ca^{2+} provided by cementing solution to form the $CaCO_3$. It has already been used in the aspect of soil reinforcement (Gitanjali et al., 2024; Wang et al., 2023a), dust suppression (Miao et al., 2024), cultural relics restoration (Dong & Liu, 2022) and heavy metal ion solidification (Li et al., 2022). The EICP technology has the advantage of limited pollution, limited disturbance and good fluidity. It should be a potential technology for soil permeability reduction because the generated $CaCO_3$ would fill the pore to reduce the permeability property (Cui et al., 2021).

The EICP technology has been initially used for soil strength improvement (Martin et al., 2021; Yang et al., 2024). Some limited attention has been gradually paid to the permeability reduction for soil. The EICP technology has been demonstrated to have an effect on permeability reduction for sandy soil. The permeability could be reduced by one order of magnitude compared with the untreated sample (Cui et al., 2024; Liu et al., 2024). Then, the relationship between the permeability and attached $CaCO_3$ was established in linear form (Cui et al., 2024) and non-linear form (Ahenkorah et al., 2021). Further studies have been conducted on the factors that influence the EICP process, which would have an influence on the treatment effect. The related research mainly focused on the strength improvement of soil. The influence factors for the EICP process could be divided into three aspects, including reaction environment, treatment method and characteristics of the soil (Lai et al., 2024). To be specified, some researchers conducted a series of experiments to investigate the treatment effect in different conditions, including cementing solution concentration (He et al., 2023), temperature (Dilrukshi et al., 2018) and PH value (Lai

* Corresponding author.
E-mail address: zjw101_0@163.com (J. Zhang).

https://doi.org/10.1016/j.bgtech.2025.100196
Received 22 April 2025; Received in revised form 24 June 2025; Accepted 20 July 2025
Available online 21 July 2025
2949-9291/© 2026 The Authors. Publishing services by Elsevier B.V. on behalf of KeAi Communications Co. Ltd. This is an open access article under the CC BY license (http://creativecommons.org/licenses/by/4.0/).

et al., 2023). These studies gave some insight into the suitable conditions to achieve the largest improvement of strength parameters. Other researchers paid attention to the influence of treatment methods, including the injection method (Zhang et al., 2022) and the mixing method (Pan et al., 2020; Cheng & Shahin, 2016). In addition, more attention has been paid to the influence of soil characteristics, including grain composition (Sun et al., 2020), particle size (Chen et al., 2023a) and compaction degree (Naeem et al., 2024). The compaction degree, which could be represented as dry density, was always used in the engineering application. The dry density would influence the seepage characteristic in the soil.

The seepage characteristic would have a certain influence on the treatment effect, especially the permeability reduction effect treated by injection method. Limited attempts have been conducted to reveal the permeability parameter of the EICP-treat soil under different initial dry densities (Mehmood et al., 2024). For example, the influence of dry density was initially investigated for the calcareous sand (Chen et al., 2023b) and loess soil (Sun et al., 2021). Meanwhile, these studies mainly regard permeability as a property that reflects the treatment effect instead of investigating the mechanism of the permeability reduction process, which would be beneficial in evaluating the permeability reduction effect under different dry densities. The permeability variation should be explained from the pore characteristic variation, which could be regarded as the micro performance of the variation of the permeability parameter (Diel et al., 2019; Koestel et al., 2020). The pore structure inside the soil has been reflected effectively by some imaging technologies, including optical microscopy, scanning electron microscopy (SEM), focused ion beam nanotomography (FIB-nt), et al. (Zachara et al., 2016; Thotakuri et al., 2024). The SEM has been used to reflect the pore characteristic to explain the variation mechanism of physical-mechanical dynamic parameters (Chen et al., 2019). Moreover, more efforts have been made to interpret the seepage-related parameter variation (Bultreys et al., 2016). To be specified, the pore image has been used to investigate the water-holding capacity and infiltrability of the soil influenced by biocrust function (Sun et al., 2023). The SEM image was quantified to investigate the saturate permeability variation of remolded loess with different dry densities (Xu et al., 2020). The above study indicated that the pore-related image could be a potentially effective method to investigate the permeability variation of EICP-treated modified silt influenced by different initial dry densities.

In this study, the influence of dry density on the permeability reduction effect was conducted for the silty sand with relatively low permeability, which was not given enough attention in the former study. The permeability reduction effect was evaluated by the saturated hydraulic conductivity and the mass of induced $CaCO_3$. The relationship variation between the above two parameters was discussed. Then, the pore characteristic, obtained by the quantified treatment of SEM image, was used to explain the permeability variation of EICP-treated soil influenced by the initial dry density. The pore characteristic was described in three aspects: area distribution, size distribution, and orientation distribution. Finally, the generalized mechanism was proposed for the permeability reduction of EICP-treated soil influenced by initial dry density.

2. Material and method

2.1. Experimental material

The soil used in this study was taken from the Yellow River flood area in Kaifeng, Henan Province, China. The soil was obtained at the depth of 1.5 m to eliminate the influence of debris and leftover roots. The particle size distribution of soil particles was determined by Malvern Mastersizer3000 laser particle size analyzer. The result showed that the occupation of sand, silt, clay was separately 69.44%, 29.63% and 0.93% in Fig. 1A. The maximum dry density is 1.62 g/cm^3. The optimal moisture content is 13.74%. The specific gravity is 2.7. The

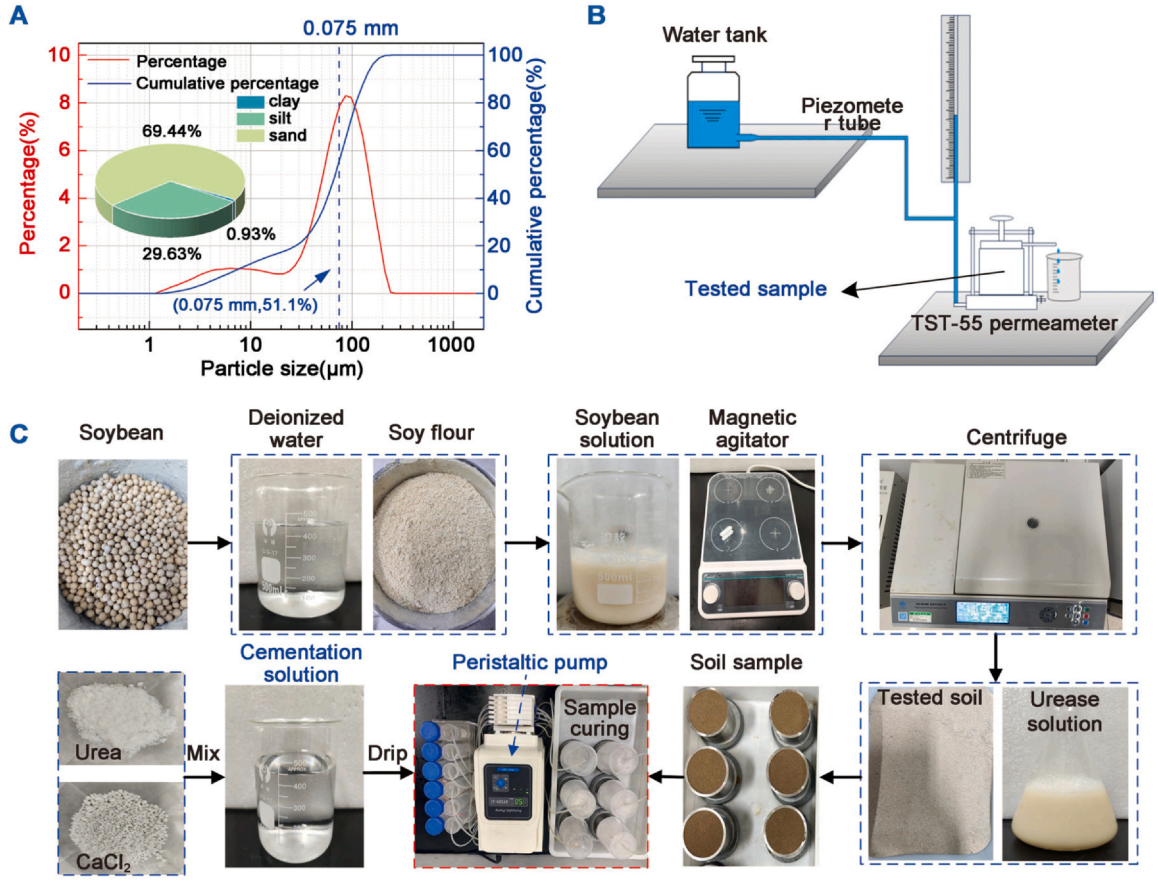


Fig. 1. Test material and procedure.

liquid limit is 25.5%. The plastic limit is 18.6%. The plasticity index is 10.9. And the uniformity coefficient is 10.53. The pH value is 6.3, and the mineral composition is mainly quartz. Fig. 1B shows a schematic diagram of the TST-55 permeameter used for measuring permeability coefficient. The falling-head method was adopted in this experiment to determine the permeability coefficient.

2.2. Specimen preparation

Fig. 1C showed the detailed procedure for the specimen preparation. Three main steps were shown, including urease solution preparation, reaction solution preparation and specimen making. The specimen was cured for 12 h in the oven with the temperature of 30 ℃.

2.2.1. Urease and reaction solution preparation

The urease solution used in the experiment was extracted from soybean which could be bought from the market. The soybean powder was obtained using the sieve with 0.5 mm for the dried soybeans crushed by a grinder. Soybean powder and deionized water were mixed at a solid-liquid ratio of 1:10 to get the mixture solution with the soybean flour concentration of 100 g/L. Then, the mixture solution was centrifuged in a high-speed centrifuge at 3999 r/min with the temperature of 4 ˚C for 15 min. The supernatant liquor was taken as the soybean urease solution. Urease activity was measured using the conductivity method (Whiffin et al.,2007). The activity of urease solution used in this experiment was 23.865 (mmol/L)/min. The cementing solution used in the experiment was composed of urea solution and calcium chloride solution with the mass ratio of 1:1. And the concentration of urea and calcium chloride solution was both 1 mol/L.

2.2.2. Specimen making

The size of soil particle used to make the specimen sample was smaller than 2 mm. The soil particle would be mixed with urease solution of 23.865 (mmol/L)/min activity. The urease solution was used to replace the water. The volume of the urease solution was controlled by achieving the optimal moisture content, which was 13.74% in this study. The specimen sample was prepared in the cutting ring with the height of 40 mm and diameter of 61.8 mm. Then the cementing solution was injected into the specimen with the peristaltic pump with the rate of 1 mL/min. The volume of injected cementing solution was 50 mL in every treatment round. The treated specimen was cured in the oven with the temperature of 30 ℃ in every treatment round.

2.2.3. Experiment condition

The experimental conditions are shown in Table 1. Five experiment groups with thirty conditions were designed in this study. Two influence factors were considered, including initial dry density and treatment times. The initial dry density considered in this study was separately 1.40, 1.45, 1.50, 1.55 and 1.60 g/cm^3, due to the maximum dry density of the soil used in this experiment being 1.62 g/cm^{3}and the requirements for compaction degree in practical engineering applications. The treatment time was separately 1, 2, 3, 4, 5, and 6. The other experiment condition has been already illustrated in the above section.

2.3. Test parameter and method

2.3.1. Saturated hydraulic conductivity

The saturated hydraulic conductivity, represented as K_{sat}, was tested by the variable water level method. The model number of the tested apparatus was TST-55 (Gao et al., 2018; Cuisinier et al., 2011). The detailed steps were referred to the *Standard for geotechnical testing method* (GB/T50123–2019). The temperature was maintained at 20 ˚C during the hydraulic conductivity test (Zhang et al., 2015; Chapuis, 2012). The K_{sat} could be calculated by the Eq. (1).

$$K_{sat}=2.3\times\frac{aL}{At}\lg\left(\frac{H_1}{H_2}\right) \tag{1}$$

The parameter a represents the cross-sectional area of the variable head tube (cm^2); the parameter L represents seepage path length (cm); the parameter A represents the section area of the sample (cm^2); the parameter t represents the test time (s); the parameter H_1 represents the hydraulic head at the beginning of the test (cm); the parameter H_2 represents the hydraulic head at the end of the test (cm).

2.3.2. The content of $CaCO_3$

The content of induced $CaCO_3$ was tested by the picking method. The content of $CaCO_3$ was calculated by the average value of the four samples taken in four layers from top to bottom divided evenly. Each of the sample was around 15 g, which was named as m_1. Then the sample was put into the dilute hydrochloric acid with the concentration of 1 mol/L until the bubble would not emerge. Then the left soil particle was put into the deionized water for 24 h. And then it would be dried and weighted. The mass was named as m_2. Then the content of $CaCO_3$ (C_{CaCO_3}) could be calculated by the Eq. (2).

$$C_{CaCO_3}=\frac{m_1-m_2}{m_2} \tag{2}$$

2.3.3. Micro-scale test

The SEM method was used to investigate the pore variation from the micro-scale test. The magnification time was 300. The SEM images were processed using Image J software. The detailed conduct steps included image preprocessing, image segmentation and parameter extraction. Four degree of the pore was classified from the conducted image, including macropore ($>$ 200 μm), mesopore (20–200 μm), small pore (5–20 μm) and micropore ($<$ 5 μm). The color representing the four degree of the pore was separately blue, green, cyan and red. The SEM image was analyzed from three perspective, including pore area distribution, pore size distribution and pore orientation distribution. The first two parameter could be obtained from the treatment by Image J software directly. The pore orientation distribution was described by the orientation probability entropy, which was represented by H_m (Chen et al., 2019). The parameter H_m was calculated by Eq. (3).

$$H_m=-\sum_{i=1}^{n}P_i\log_n P_i \tag{3}$$

where P represents the probability that the pore area occurs within a specific angle range; n is the number of equally divided areas divided by angles, the value was 18 in this study. The value of H_m is between 0 and 1. And the pore structure is less ordered as H_m increases.

Table 1
Experimental program of EICP test.

Specimen ID	Urase activity/ ((mmol/L)/min)	Cementing solution concentration/(mol/L)	Dry density/ (g/cm^3)	Treatment times, n
A1–A6	23.86	1.00	1.40	1,2,3,4,5,6
B1–B6	23.86	1.00	1.45	1,2,3,4,5,6
C1–C6	23.86	1.00	1.50	1,2,3,4,5,6
D1–D6	23.86	1.00	1.55	1,2,3,4,5,6
E1–E6	23.86	1.00	1.60	1,2,3,4,5,6

3. Result and discussion

3.1. Saturated hydraulic conductivity and induced $CaCO_3$ mass

Fig. 2A shows the variation of saturated hydraulic conductivity (represented as K_{sat}) under different treatment times and dry density of untreated soil. It could be found that the K_{sat} would have a general decrease trend with the treatment time in the five dry densities of untreated soil. The decrease degree would obviously be large after one treatment time. It should be noted that the permeability of untreated soil would have a slight decrease when the dry density increased from 1.55 g/cm^3 to 1.60 g/cm^3. This indicated that the pore volume might decrease slightly when the dry density was larger than 1.55 g/cm^3. The value of K_{sat} would have a relatively great decrease with one treatment time when the dry density was between 1.40 and 1.55 g/cm^3. Three typical variation types could be concluded for the relationship between K_{sat} and treatment time. The first typical type was K_{sat} variation when the initial dry density was 1.40 g/cm^3, which could represent the untreated soil was under loose conditions. There would be three decrease stages during the six treatment times. The decrease value would be the largest after one treatment time. It would have a moderate decrease in value when the treatment time changed from 1 to 3. The decreased value would further have a decrease when the treatment time was larger than 4. The second typical type was K_{sat} variation when the initial dry density was from 1.45 to 1.55 g/cm^3, which could represent the untreated soil under relatively dense conditions.

There would only be two stages of decrease during the six treatment times. The decreased value of K_{sat} would change to a much smaller value when the treatment time changed to 2. The third typical type was K_{sat} variation when the initial dry density was 1.60 g/cm^3, which could represent the untreated soil under dense conditions. The main difference from the second typical type was that the decreased value of the two stages only had a small gap. The three typical types exhibited the variation of the permeability reduction process with the initial dry density. Generally speaking, the initial dry density would have a negative influence on the permeability decrease value. The decreased value would have a decreasing trend with the treatment time. Furthermore, it could be inferred that the decreased value could be maintained at a certain small value when the density reaches a certain value, which could be represented by a similar decrease trend after three treatment times in all five densities. At the same time, the decreased trend was slight when the dry density was 1.60 g/cm^3. Some further investigation was given to the parameter $^{\triangle}K_i$, which represented the difference of K_{sat} between untreated and the i time treatment. Fig. 2B shows the variation of $^{\triangle}K_i$ with dry-density. It could be found that the $^{\triangle}K_i$ would all have a decreasing trend with treatment time in the five dry density conditions. It should be noticed that the decrease rate of $^{\triangle}K_i$ would be relatively uniform with the dry density after one treatment time. The decrease rate of $^{\triangle}K_i$ would be gradual with dry density after one treatment time. This indicated that the dry density would have a relatively obvious influence on the treatment effect at the beginning of the treatment process. The influence would be weakened by the increase in treatment time.

Fig. 2C showed that the induced $CaCO_3$ would have an increased trend with the treatment in general. The variation of C_{CaCO_3} obeyed a relatively uniform increase with the treatment time. It should be noticed that the decrease trend was not uniform with the treatment time, which was shown in Fig. 2A. This indicated that the function degree of induced $CaCO_3$ would vary with the treatment time. This might also be the evidence that the seepage characteristic (advantage or uniform)

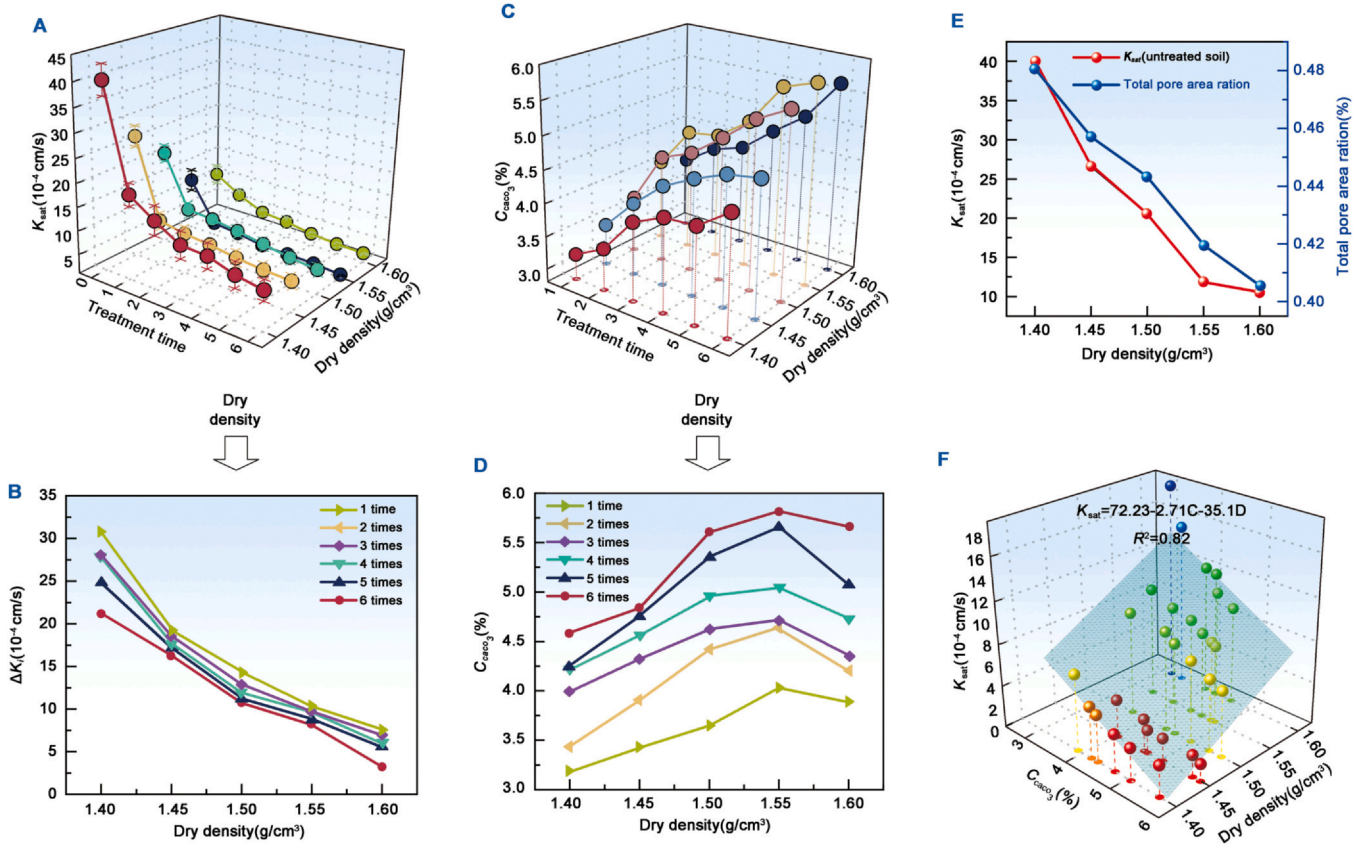


Fig. 2. (**A**) The variation of saturated hydraulic conductivity under different dry density and treatment time; (**B**) The variation patterns of $^{\triangle}K_i$ under different dry densities; (**C**) The variation of induced $CaCO_3$ content under different dry density and treatment time; (**D**) Variation patterns of C under different dry densities; (**E**) The relationship between permeability coefficient and total pore area under different dry densities for untreated soils; (**F**) The relationship between saturated hydraulic conductivity, induced $CaCO_3$ content and different dry density.

would vary during the treatment process, which would directly decrease the value of K_{sat} and the treatment effect. Fig. 2D showed the relationship between C_{CaCO_3} and dry density under different treatment time. It could be found that the C_{CaCO_3} would all have an increase and then decrease trend with the dry density changed from 1.40 to 1.60 g/cm^3. The maximum of C_{CaCO_3} would appear when the dry density was 1.55 g/cm^3 in all the six different treatment time. This indicated that there would exist a certain condition of untreated soil, which would be the most beneficial for the generation and attachment of $CaCO_3$. Some interpretation would be given to this phenomenon. The soil was in loose condition when the dry density was 1.40 g/cm^3. The seepage channel was large because of the macropore existing among the soil particle in this condition. The attachment of induced $CaCO_3$ would be relative difficult in the macropore, although the solution could flow in the soil sample easily (Wang et al., 2023b). Thus, the $CaCO_3$ remained in the soil was relatively little, which could be benefit for the hydraulic conductivity reduction. Part of the macropore would be reduced to smaller pore with the increase of dry density, which could be more benefit for the attachment of induced $CaCO_3$. This might be the reason for increase trend of induced $CaCO_3$ when the dry density increased from 1.40 to 1.55 g/cm^3. It should be noticed that the attached $CaCO_3$ decreased when the dry density changed from 1.55 to 1.60 g/cm^3. This would prove the above interpretation for the reason that the treatment effect was better when the dry density was 1.55 g/cm^3 compared with the density of 1.60 g/cm^3 in Fig. 2F. It could be further inferred that the amount of attached $CaCO_3$ and the seepage characteristic would both have influence to the treatment effect of soil.

An interesting could be found that the treatment effect for untreated soil with a dry density of 1.55 g/cm^3 was better than the 1.60 g/cm^3. Some discussion was given by considering the untreated soil characteristics. The variation of K_{sat} and total pore area ratio with dry density for untreated soil was shown in Fig. 2F. It could be found that the total pore area ratio would have an obvious decrease when the dry density changed from 1.55 to 1.60 g/cm^3. Meanwhile, the value of K_{sat} would only have a slight decrease. This might indicate the seepage characteristic would be different between the untreated soil under the dry density of 1.55 and 1.60 g/cm^3. To be specified, the seepage condition would have the advantage characteristic when the dry density was 1.55 g/cm^3, which indicated that the seepage might mainly occur in the large channels. The value of K_{sat} was mainly determined by the local seepage area. The seepage characteristic would change to relative uniform when the dry density was 1.60 g/cm^3 in a dense condition. The area where seepage occurs would be wider, but the local seepage channel would be smaller. The different seepage characteristic might respond for the different treatment result. The solution could be easier to seepage into the treated soil through the relatively large channel when the dry density was 1.55 g/cm^3. The local seepage velocity would be relatively small, which would be beneficial for the attachment of induced $CaCO_3$. While the local seepage velocity would be relatively large because of the smaller local seepage channel. This would not benefit the attachment of induced $CaCO_3$. A linear relationship was established for the parameter of K_{sat}, C_{CaCO_3} and dry density, which was shown in Fig. 2F. The fitting result was $K_{sat} = 72.23\text{-}2.71C_{CaCO3}\text{-}35.1\rho_d$. This indicated that the permeability of treated soil would be influenced by both C_{CaCO_3} and dry density obviously. And the dry density and induced $CaCO_3$ mass would have the negative influence to the permeability of treated silty sand.

3.2. Pore area and size distribution

Fig. 3A shows the four pore types in the soil under different dry densities before and after the six times bio-treatments from the qualitative perspective. The macropore, represented in the color of blue, would have an obvious decrease trend with the increase of dry density before the treatment. This indicated that the seepage characteristic might vary with the dry density, which would also have an influence on the bio-treatment process. It could also be found that the occupation of macropores would decrease after the bio-treatment in all five dry densities. It should be pointed out that the macropore would not exist after the bio-treatment time when the dry density was 1.55 and 1.60 g/cm^3. And there would still exist the macropore after the bio-treatment when the density was 1.40, 1.45 and 1.50 g/cm^3. It could also be found that the mesopore, represented by the color green, would have an increased trend in all five conditions. The small pore and micropore, represented separately by cyan and red, would not have obvious variation in the five conditions. The above variation indicated that the decrease of K_{sat} would be mainly caused by changing the macropore to mesopore from the perspective of pore variation.

Some quantitative evaluation was given to the occupation of the four types of the pore before and after the bio-treatment, which was separately shown in Fig. 3B. It could be found that the total pore area would have a near-linear decrease with the dry density both before and after the bio-treatment. To be specified, the total pore area occupation decreased from 48.09% to 40.55% when the dry density changed from 1.40 to 1.60 g/cm^3 before the treatment. The decrease value was 7.54%. The total pore area occupation decreased from 45.68% to 37.63% when the dry density was low after the bio-treatment. The decreased value was 8.05%, which was only a small larger than the value before treatment. This indicated that the decreased function for the parameter K_{sat} by the initial dry density was larger than bio-treatment. More detailed information about the decrease value of the pore after the bio-treatment was summarized in Table 2. It could be found that the decrease value of the total pore would have the increase and then decrease variation with the increase of dry density. The maximum decrease value was in the dry density of 1.55 g/cm^3. This variation was consistent with the parameter K_{sat}. This proved that the total pore variation was the crucial factor for the general decrease trend of parameter K_{sat}.

More attention was paid to the variation of three specific pore types, including macropore, mesopore, small and micropore. The macropores would all have a decrease trend in all five dry densities. Meanwhile, the mesopore region will show an increased trend. Small and micropores would also show a decreasing trend. It could be inferred that the seepage mainly occurred in the large and mesopores (Xu et al., 2021). Thus, the induced $CaCO_3$ would mainly attach in the large and mesopore. The attached $CaCO_3$ would reduce the size of the pore. It should also be pointed out that the size of the induced $CaCO_3$ would also be different because of the different attachment environments. The moderate size of the induced $CaCO_3$ might reduce the macropore to the mesopore. The large size of the induced $CaCO_3$ might clog the large mesopore. And the small size of induced $CaCO_3$ might change the mesopore to a small micropore. More analysis should be given, combined with the pore size distribution characteristic, which will be discussed in detail in the next section. It should also be pointed out that the pore variation degree was much smaller when the dry density was 1.45 g/cm^3 compared with other conditions. This might be the reason that the C_{CaCO_3} would have the most near-linear relationship with the K_{sat}.

Fig. 3C shows the pore size distribution before and after the bio-treatment under the five different densities. A cumulative graph was used to analyze the pore size distribution characteristic. It could be found that the maximum pore diameter would be reduced after the treatment in all five dry densities. The two cumulative lines would not have an intersection when the dry density was 1.40 g/cm^3. This indicated that the pore size would have an overall decreasing trend when the soil was in a loose condition The occupation of different diameters would be relatively uniform in the mesopore and macropore before the bio-treatment when the dry density was 1.40 g/cm^3. Relative uniform seepage might occur in all macropores and parts of the mesopore. The induced $CaCO_3$ might have a greater possibility to attach in the pore with two aspects. The first one was the pore with a large diameter, in which the local seepage velocity was small enough to be beneficial for

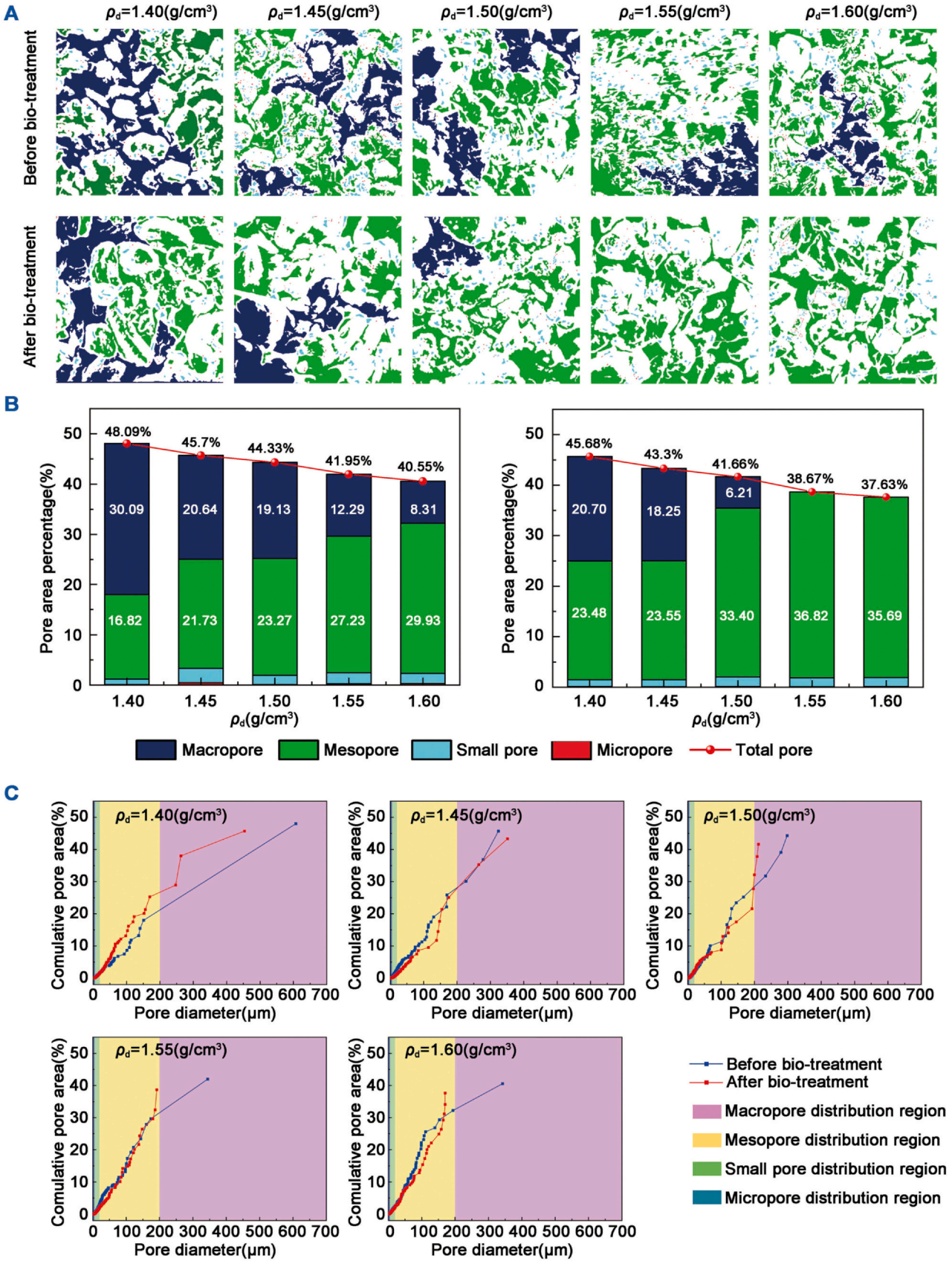


Fig. 3. (**A**) The pore area distribution for the soil under five dry densities before and after the bio-treatment: (**B**) Pore area occupation before and after treatment; (**C**) Pore size distribution before and after the bio-treatment under five different dry densities.

Table 2
The detailed information about the pore variation.

Dry density (g/cm^3)	Decrease value (%)			
	Total pore	Macropore	Mesopore	Small and micropore
1.40	2.41	9.39	−6.66	5.14
1.45	2.40	2.39	−1.82	2.97
1.50	2.67	12.92	−10.13	5.46
1.55	3.28	12.29	−9.59	5.98
1.60	2.92	8.31	−5.76	5.47

the attachment. The second one was the mesopore with a smaller diameter, which would have smaller space to benefit from the attachment. Thus, it could be found that the diameter would mainly concentrate around a certain value in the macropore after the treatment.

The maximum pore diameter would not have an obvious change after the bio-treatment when the dry density was 1.45 g/cm^3, which would be different from the other four conditions. The seepage characteristic was also relatively uniform in this condition. It should be noticed that the maximum diameter was similar to the soil after bio-treatment under the dry density of 1.40 g/cm^3, which was inferred to be not beneficial for the $CaCO_3$ attachment. Thus, the $CaCO_3$ would mainly attach in the mesopore when the dry density was 1.45 g/cm^3. The maximum diameter would be relatively smaller when the dry density was 1.50 g/cm^3, compared with the 1.45 g/cm^3. The uniform seepage would also occur at the beginning of the treatment. The $CaCO_3$ would attach in the mesopore at the beginning. Then, it could be inferred that the seepage characteristic would change to relatively non-uniform with treatment time. Thus, the largest diameter would decrease in this condition. It should be pointed out that the variation of the pore diameter mainly occurred in the macropore when the dry density was 1.55 g/cm^3, which would be the demonstration for the statement of Section 3.1. The pore diameter variation of 1.60 g/cm^3 dry density was similar to the 1.55 g/cm^3. The only difference was that the mesopore would have variation after the bio-treatment when the dry density was 1.60 g/cm^3. Some explanation should be given from the perspective of pore orientation distribution in Section 3.3.

3.3. Pore orientation distribution

Fig. 4 shows the pore directional distribution characteristics before and after the bio-treatment under the five dry densities. It could be found that the pore orientation would have an advantage direction when the dry density was relatively small before the treatment, e.g. 1.40, and 1.45 g/cm^3. The characteristic of advantage orientation might be beneficial for the connectivity of the pore. This might also be a reason for the large value of K_{sat} when the soil was in loose condition. The pore orientation would be scattered when the dry density was relatively large before the treatment, e.g., 1.55 and 1.60 g/cm^3. The scattered distribution of pore orientation might not benefit the connectivity of the pore, which would reduce the permeability of the soil. It could be found that the pore directional distribution would become more scattered after the bio-treatment. The variation characteristic would be influenced by the initial dry density. To be specified, the pore directional distribution would change from one to several advantage orientations when the initial dry density was 1.40 and 1.45 g/cm^3. The pore directional distribution seemed to not have obvious variation in the advantage orientation when the initial dry density was 1.55 and 1.60 g/cm^3 after the bio-treatment. This was mainly because of the scattered orientation distribution of the untreated soil. Thus, it could be inferred that the bio-treatment would make the orientation distribution to be more scattered when the soil was under relatively loose conditions, which would contribute to reducing the connectivity of the pore to decrease the value of K_{sat}.

The parameter H_m was used to quantitively evaluate the pore orientation distribution, which is shown in Table 3. The value of H_m would increase from 0.30 to 0.78 after the bio-treatment when the dry density was 1.40 g/cm^3. And it increased from 0.33 to 0.73 when the dry density was 1.45 g/cm^3. The above two variation trends of H_m could be clearly reflected in the above rose diagrams. More attention would be given to the variation trend of pore directional distribution reflected by the parameter H_m under the other three dry densities. The value of H_m increased from 0.45 to 0.72 when the dry density was 1.50 g/cm^3. It increased from 0.72 to 0.94 when the dry density was 1.55 g/cm^3. And it increased from 0.76 to 0.80 when the dry density was 1.60 g/cm^3. It should be pointed out that the H_m would be the largest with the value of 0.94 after the bio-treatment when the dry density was 1.55 g/cm^3. The treatment effect was the best among the five dry densities. This indicated that the scattered pore orientation distribution would also contribute to the permeability reduction effect in the bio-treatment process. It should also be pointed out that the value of H_m in the dry density of 1.55 g/cm^3 was larger than the value in the 1.60 g/cm^3. This would be the reason for that the treatment effect would be better in the dry density of 1.55 g/cm^3, although the pore size would be generally smaller in the dry density of 1.60 g/cm^3.

3.4. Generalized mechanism for permeability reduction influenced by dry density

The generalized mechanism was illustrated by combining it with the non-uniform seepage theory in the soil. The non-uniform seepage theory has been gradually used to analyze the phenomenon related to seepage in the soil. For example, Šimůnek et al. (2003) stated that preferential and non-uniform transport of water could occur at any seepage scale. Soto-Gómez et al. (2020) demonstrated that the properties of the backbone would be considered for understanding the macropore flow and the preferential transport of solutes and colloids. Besides, the technology of CT has been widely used to reveal the non-uniform characteristics in the soil (Katuwal et al., 2015; Li & Tang, 2019; Zhang et al., 2017). Those studies demonstrated that the non-uniform seepage theory would be helpful to explain some phenomena that could hardly be interpreted by traditional uniform seepage theory. Fig. 5 gives a summarize to the treatment process from three perspectives to reveal the influence of the dry density, including the pore condition before treatment, general characteristic during treatment and the treatment effect. The soil condition would change from loose to dense before the bio-treatment with the dry density increase (Fig. 5A). The occupation of macropores and diameter of the largest pores would decrease when soil conditions change from loose to dense. Besides, the complex of pore orientation would have an increased trend with the dry density. The initial pore condition would have an influence on the seepage characteristic during the treatment, which might be the main aspect of interpreting the influence of the dry density on the treatment effect. Some inferences would be given based on the above investigation of the variation of K_{sat} and pore characteristics. The general characteristic variation during the treatment was illustrated in three aspects, including general seepage characteristics, the process of induced $CaCO_3$ attachment and pore orientation distribution. The detailed information is shown in Fig. 5B. The variation of treatment effect influenced by the dry density is shown in Fig. 5C. The treatment effect was represented by relative K_{sat}, which was calculated by dividing the K_{sat} after the treatment by the value before the treatment. The compaction degree was used to give a direct connection with the engineering application. The compaction degree (D_c) was calculated by the dry density (ρ_d) with the equation $D_c = \frac{\rho_d}{\rho_{d\,max}} \times 100\%$.

Loose condition: Uniform seepage would occur in both macropores and mesopores when the soil was in the loose condition. It could be inferred that the local velocity would all be small enough, although the seepage velocity distribution was non-uniform in the whole sample. The

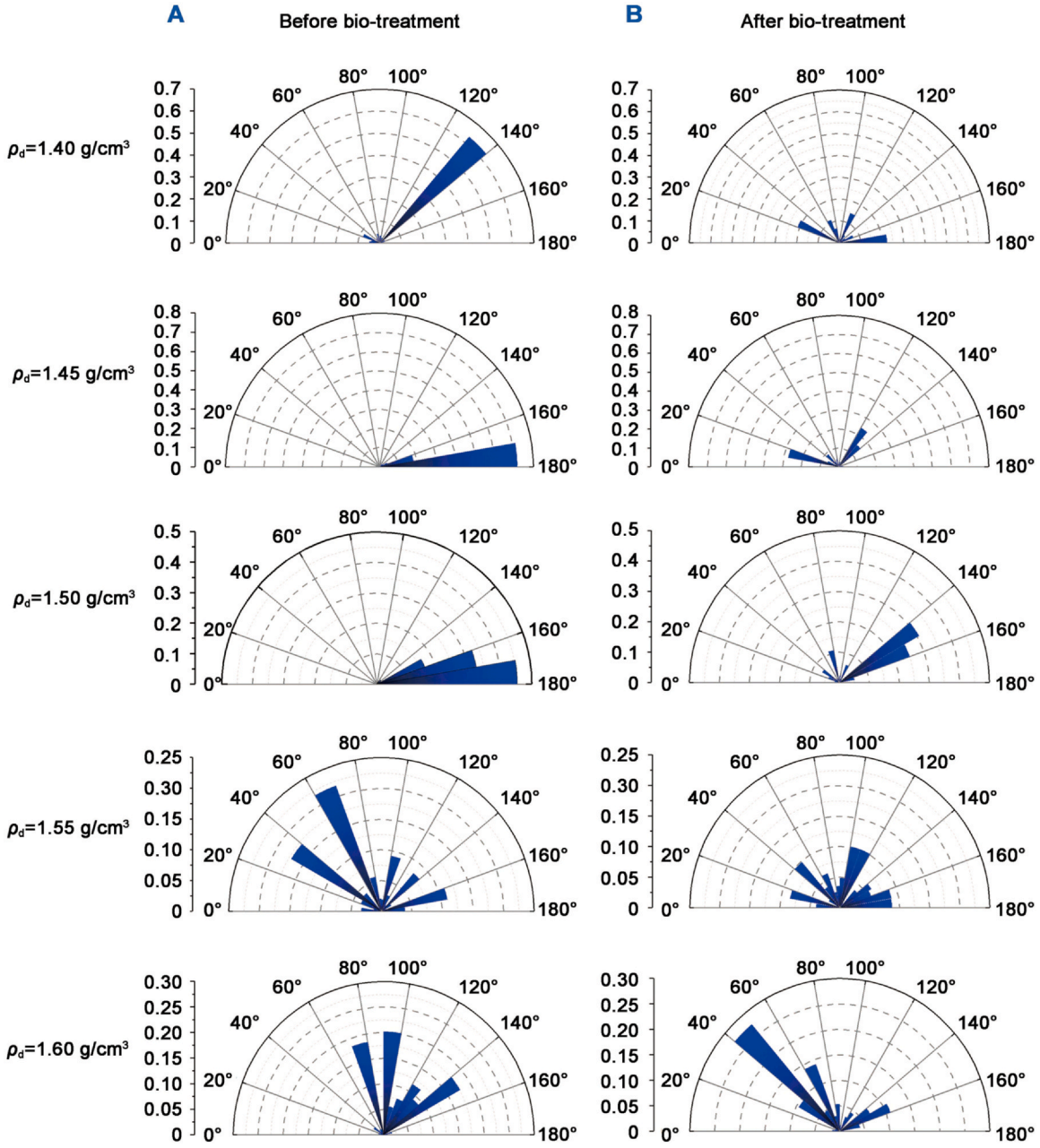


Fig. 4. Rose diagrams of the pore orientation distribution under different dry density: (**A**) Before bio-treatment; (**B**) After bio-treatment.

Table 3
The directional probability entropy (H_m) before and after the bio-treatment.

ρ_d/(g/cm^3)	1.40	1.45	1.50	1.55	1.60
The value of H_m before treatment	0.30	0.33	0.45	0.72	0.76
The value of H_m after treatment	0.78	0.73	0.72	0.94	0.80

$CaCO_3$ would attach both in macropore and mesopore uniformly. Besides, it should be pointed out that the pore orientation was relatively uniform before treatment, which would contribute to the connectivity between the pores. The attached $CaCO_3$ would greatly change the pore orientation characteristic from advantage to complex which would be another reason for the permeability reduction, except for the filling function of induced $CaCO_3$. The dry density of 1.40–1.50 g/cm^3 might be included in this condition, which indicated the compaction degree was smaller than 90%. The treatment effect would decrease with the compaction degree.

Relative dense condition: The advantage seepage characteristic would gradually merge with the increase of dry density, indicating the variation of the soil condition change from loose to relatively dense. This was mainly because of the variation in pore characteristics. To be specific, the pore size might mainly concentrate on two certain levels, although the general pore diameter would have a decreasing trend. Then, the $CaCO_3$ would preferentially attach to the pore in the advantage seepage channels. The pore orientation characteristic would also be changed to complex after treatment time. While the variation rate would decrease with the increase of dry density. The dry density of 1.55 g/cm^3 might be included in this condition, which indicated the compaction degree was about 95%. The treatment effect would increase with the compaction degree. The dry density of 1.50 g/cm^3 might be the transition stage between the loose and relatively dense conditions.

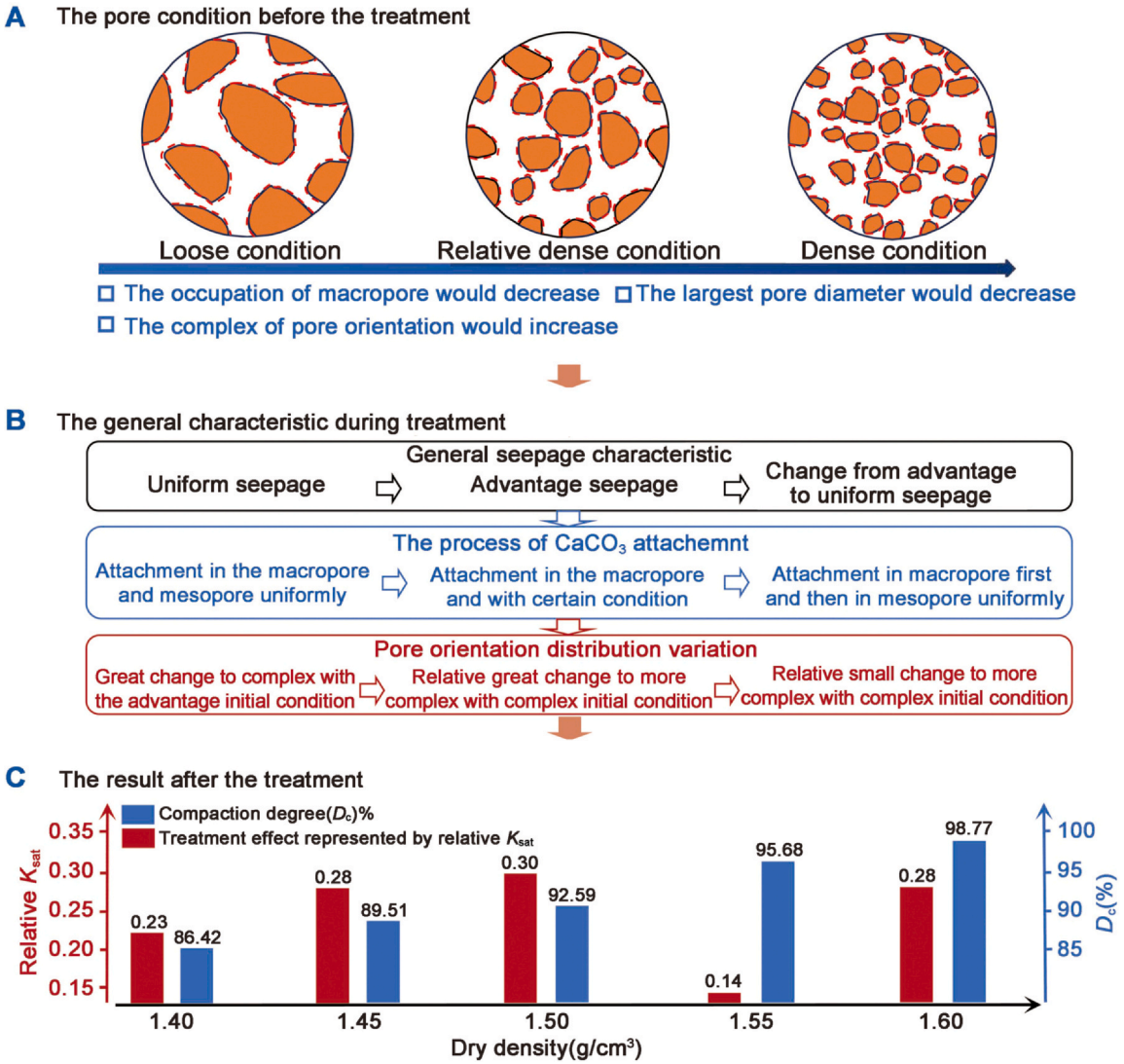


Fig. 5. The general mechanism graph for the variation by dry density.

It should be pointed out that the dry density corresponding to the best treatment effect was in this condition, which might be around 1.55 g/cm^3 in this study.

Dense condition: The seepage characteristic would change from advantage to uniform in this condition during the bio-treatment process. To be specified, the seepage would occur in the macropore at the initial stage. Thus, the induced $CaCO_3$ would preferentially attach to these pores. Then, the macropore might all be changed to the mesopore. The uniform seepage would merge in the mesopore. The attachment of induced $CaCO_3$ would be uniform. It should be noticed that the amount of injected cementation solution would be limited because of the low permeability in the mesopore. Thus, the reduction function would be limited. In other words, the reduction of K_{sat} would mainly occur in the advantage seepage phase. Thus, the degree of variation in the pore orientation distribution characteristic would decrease. The treatment effect would also decrease compared with the relatively dense condition. The 1.60 g/cm^3 was included, corresponding to a compaction degree of about 99%.

3.5. Comparison and discussion

The above analysis gave a detailed description of the variation of K_{sat} and C_{CaCO_3} under different initial dry densities. Here, some comparisons were made with former studies (Fig. 6). The soil in the study of Chen et al. (2023b) was calcareous sand, which could represent the soil with relatively high permeability. The soil in the study of Sun et al. (2021) was loess soil, which could represent the soil with relatively low permeability. It could be found the value of K_{sat} would have a general decrease trend with dry density for the calcareous sand and loess soil. Meanwhile, there would be a decrease and then an increase trend with the dry density in our study. It should be pointed out that the permeability order from highest to lowest was calcareous sand, silty sand in this study, and loess soil. This indicated that the permeability reduction effect would keep a continuous increase trend when the soil gradation was poor and concentrated in the large particle size range, e.g., sand. Meanwhile, the permeability reduction effect would first increase and then decrease with the increase of dry density when the soil gradation was relatively good and in the small particle size range, e.g., silty sand. It should be noticed that the value of K_{sat} would have no increasing trend in loess soil, whose permeability was smaller than the silty sand in our study. The variation pattern might not be fully exhibited with only three dry densities considered. The increased trend could not be found, which might be caused by the absence of the data when the dry density was 1.55 and 1.65 g/cm^3.

The variation of C_{CaCO_3} under different dry densities was also compared, which was shown in Fig. 6. It could be found that the increase degree and rate were obviously larger when the soil gradation was poor and concentrated in the large particle size range. The variation of C_{CaCO_3}

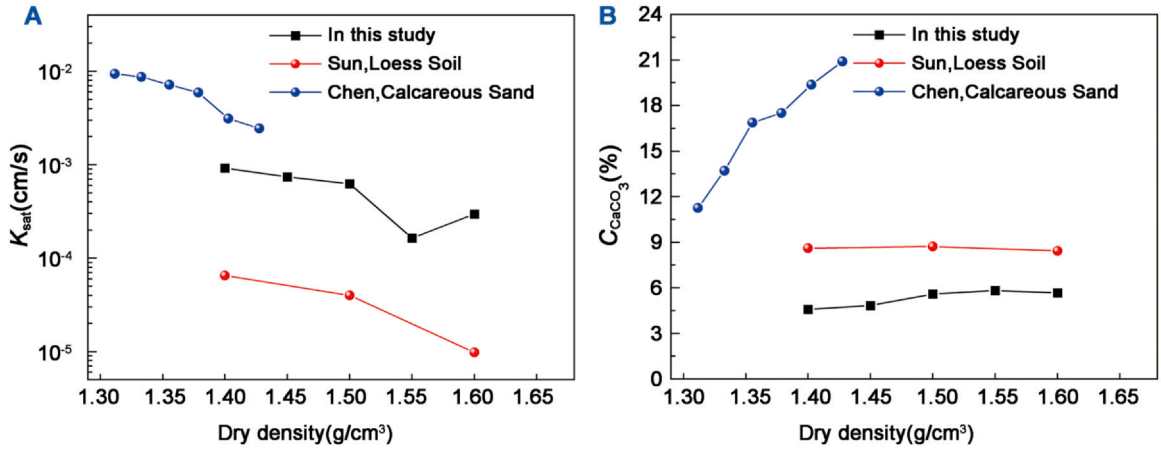


Fig. 6. Treatment effect comparison with former similar studies.

would correspond to K_{sat}. This might indicate that the mass of induced $CaCO_3$ would be the key factor in this condition. Besides, the variation of C_{CaCO_3} would prove that the large pore space would benefit the generation of $CaCO_3$ (Wang et al., 2023b). The variation degree and rate would be obviously small when the soil gradation was relatively good and in the small particle size range, e.g., loess soil and silty sand. However, there would be a variation of one magnitude order for K_{sat} under the above two conditions, which would not correspond to the C_{CaCO_3}. This might also be indirect evidence that the distribution characteristic would have an obvious influence on the permeability reduction effect in the soil with relatively low permeability. The above statement indicated that the mechanism of influence for the reduction of permeability by dry density would be changed with the variation of initial soil permeability.

4. Conclusion

Some detailed investigation was given to treatment effect by EICP technology for the silty sand soil in different initial dry density. The treatment effect was evaluated by the saturated hydraulic conductivity (K_{sat}) and induced $CaCO_3$ (C_{CaCO_3}). The relationship between K_{sat} and C_{CaCO_3} was investigated under different dry density. Furthermore, a deep discussion was given to the treatment mechanism from the perspective of pore variation by using the SEM image. The following conclusions were proposed.

(1) The EICP technology could be effectively used in permeability reduction for the silt soil. The permeability of treated soil would have a decrease and then increase trend with the increase of dry density. And the induced $CaCO_3$ would have corresponding variation trend. The treatment effect would be the best around the dry density of 1.55 g/cm^3. The content and distribution characteristic of induced $CaCO_3$ would both have the influence to the treatment effect.
(2) The total pore area would have a near linear decrease trend with dry density both before and after the treatment. The macropore variation would have the mainly contribution to the treatment effect. The macropore would not exist after the treatment when the dry density was larger than 1.55 g/cm^3. The largest pore diameter first decreases then increases with dry density before bio-treatment. It shows a consistent decreasing trend with dry density after treatment. And the bio-treatment would change the pore orientation to more complex.
(3) The generalized variation mechanism of treatment process influenced by the dry density was proposed based on the variation of permeability parameter and pore characteristic. The general seepage characteristic would successively undergo three conditions with the increase of dry density, including uniform, advantage and advantage to uniform. The different seepage characteristic would lead to the different $CaCO_3$ attachment process.

CRediT authorship contribution statement

Lei Shi: Writing – review & editing, Writing – original draft, Visualization, Validation, Supervision, Resources, Methodology, Investigation, Funding acquisition, Formal analysis, Data curation, Conceptualization. **Jianwei Zhang:** Supervision, Resources, Investigation, Funding acquisition, Formal analysis, Conceptualization. **Xiangchun Xu:** Validation, Supervision, Software, Methodology, Data curation. **Jiaming Fang:** Writing – original draft, Visualization, Supervision, Methodology, Investigation, Data curation, Conceptualization. **Huan Zhang:** Writing – review & editing, Writing – original draft, Software, Resources, Project administration, Methodology, Investigation, Formal analysis, Data curation, Conceptualization.

Declaration of Competing Interest

The authors declare that have no known competing financial interests or personal relationships that could have appeared to influence the work reported in this paper.

Acknowledgements

This work was supported by the China Postdoctoral Science Foundation Funded Project (No. 2021M701083), Key Scientific and Technological Projects of Henan Province (No. 232102321141) and Joint Fund of Technical R&D Program of Henan Province (No. 225200810005), Key Research Projects of Higher Education Institutions in Henan Province (24A560003). The authors would like to thank the editors and anonymous reviewers for their valuable comments and suggestions that significantly helped improve the mass of this paper.

References

Ahenkorah, I., Rahman, M. M., Karim, M. R., & Beecham, S. (2021). Enzyme induced calcium carbonate precipitation and its engineering application: A systematic review and meta-analysis. *Construction and Building Materials, 308*, Article 125000. https://doi.org/10.1016/j.conbuildmat.2021.125000

Bultreys, T., De Boever, W., & Cnudde, V. (2016). Imaging and image-based fluid transport modeling at the pore scale in geological materials: A practical introduction to the current state-of-the-art. *Earth-Science Reviews, 155*, 93–128. https://doi.org/10.1016/j.earscirev.2016.02.001

Chapuis, R. P. (2012). Predicting the saturated hydraulic conductivity of soils: A review. *Bulletin of Engineering Geology and the Environment, 71*(3), https://doi.org/10.1007/s10064-012-0418-7

Chen, Y., Chai, S., Cai, D., et al. (2023a). Experimental study on shear mechanical properties of improved loess based on rubber particle incorporation and EICP technology. *Frontiers in Earth Science, 11*, Article 1270102. https://doi.org/10.3389/feart.2023.1270102

Chen, H., Chen, H., Jiang, Y., Niu, C., Leng, G., & Tian, G. (2019). Dynamic characteristics of saturated loess under different confining pressures: A microscopic analysis. *Bulletin of Engineering Geology and the Environment, 78*(2), 931–944. https://doi.org/10.1007/s10064-017-1101-9

Chen, Y., Han, Y., Zhang, X., Sarajpoor, S., Zhang, S., & Yao, X. (2023b). Experimental study on permeability and strength characteristics of MICP-treated calcareous sand. *Biogeotechnics, 1*(3), https://doi.org/10.1016/j.bgtech.2023.100034

Cheng, L., & Shahin, M. A. (2016). Urease active bioslurry: A novel soil improvement approach based on microbially induced carbonate precipitation. *Canadian Geotechnical Journal, cgj-2015-0635*. https://doi.org/10.1139/cgj-2015-0635

Cui, M.-J., Lai, H. J., Hoang, T., & Chu, J. (2021). One-phase-low-ph enzyme induced carbonate precipitation (eicp) method for soil improvement. *Acta Geotechnica: An International Journal for Geoengineering, 16*(2), https://doi.org/10.1007/s11440-020-01043-2

Cui, M.-J., Lai, H. J., Wu, S. F., & Chu, J. (2024). Comparison of soil improvement methods using crude soybean enzyme, bacterial enzyme or bacteria-induced carbonate precipitation. *Géotechnique, 74*(1), 9. https://doi.org/10.1680/jgeot.21.00131

Cuisinier, O., Auriol, J. C., Borgne, T. L., & Deneele, D. (2011). Microstructure and hydraulic conductivity of a compacted lime-treated soil. *Engineering Geology, 123*(3), 187–193. https://doi.org/10.1016/j.enggeo.2011.07.010

Diel, J., Vogel, Hans-Jörg, & Schlüter, Steffen (2019). Impact of wetting and drying cycles on soil structure dynamics. *Geoderma, 345*, 63–71. https://doi.org/10.1016/j.geoderma.2019.03.018

Dilrukshi, R. A. N., A. N, Nakashima, K., & Kawasaki, S. (2018). Soil improvement using plant-derived urease-induced calcium carbonate precipitation. *Soils and Foundations, 58*, 894–910. https://doi.org/10.1016/j.sandf.2018.04.003

Dong, J., & Liu, X. (2022). Application of improved enzyme induced calcium carbonate precipitation (EICP) technology in surface protection of earthen sites. *Journal of Cultural Heritage, 54*, 146–154. https://doi.org/10.1016/j.culher.2022.01.016

Gao, Y., Qian, H., Li, X., Chen, J., & Jia, H. (2018). Effects of lime treatment on the hydraulic conductivity and microstructure of loess. *Environmental Earth Sciences, 77*(14), 1–15. https://doi.org/10.1007/s12665-018-7715-9

Gitanjali, A., Jhuo, Y. S., Yeh, F. H., & Ge, L. (2024). Bio-cementation of sand using enzyme-induced calcite precipitation: Mechanical behavior and microstructural analysis. *Construction Building Materials (Feb. 23), 417*. https://doi.org/10.1016/j.conbuildmat.2024.135360

He, J., Liu, Y., Liu, L., et al. (2023). Recent development on optimization of bio-cementation for soil stabilization and wind erosion control. *Biogeotechnics, 1*(2), Article 100022. https://doi.org/10.1016/j.bgtech.2023.100022

Katuwal, S., Norgaard, T., Moldrup, P., et al. (2015). Linking air and water transport in intact soils to macropore characteristics inferred from X-ray computed tomography. *Geoderma, 237*, 9–20. https://doi.org/10.1016/j.geoderma.2014.08.006

Koestel, J., Larsbo, M., & Jarvis, N. (2020). Scale and rev analyses for porosity and pore connectivity measures in undisturbed soil. *Geoderma, 366*, Article 114206. https://doi.org/10.1016/j.geoderma.2020.114206

Lai, H. J., Cui, M. J., & Chu, J. (2023). Effect of ph on soil improvement using one-phase-low-ph micp or eicp biocementation method. *Acta Geotechnica: An International journal for Geoengineering, 18*(6), 3259–3272. https://doi.org/10.1007/s11440-022-01759-3

Lai, H., Ding, X., Cui, M., Zheng, J., Chu, J., & Chen, Z. (2024). Factors affecting the effectiveness of biocementation of soil. *Biogeotechnics, 2*(3), https://doi.org/10.1016/j.bgtech.2024.100087

Li, Z., & Tang, L. (2019). Using synchrotron based X-ray microcomputed tomography to characterize water distribution in compacted soils. *Advances in Materials Science and Engineering, 2019*(1), Article 7147283. https://doi.org/10.1155/2019/7147283

Li, W., Zhang, Y., & Achal, V. (2022). Mechanisms of cadmium retention on enzyme-induced carbonate precipitation (EICP) of Ca/Mg: Nucleation, chemisorption, and co-precipitation. *Journal of Environmental Chemical Engineering, 10*, Article 107507. https://doi.org/10.1016/j.jece.2022.107507

Liu, L., Gao, Y., Meng, H., Pan, Q., Wang, Z., Zhou, Y., et al. (2024). Pore-scale, mechanical, and hydraulic properties of eicp-treated sand using crude legume ureases with different protein contents. *Acta Geotechnica, 19*(7), https://doi.org/10.1007/s11440-023-02211-w

Martin, K., Tirkolaei, H. K., & Kavazanjian, E. (2021). Enhancing the strength of granular material with a modified enzyme-induced carbonate precipitation (EICP) treatment solution. *Construction and Building Materials, 271*, Article 121529. https://doi.org/10.1016/j.conbuildmat.2020.121529

Mehmood, M., Guo, Y., Wang, L., Liu, Y., Uge, B. U., & Ali, S. (2024). Influence of enzyme induced carbonate precipitation (eicp) on the engineering characteristics of expansive soil. *Arabian Journal for Science and Engineering, 49*(10), 14101–14116. https://doi.org/10.1007/s13369-024-08896-9

Miao, L., Wang, H., Sun, X., Wu, L., & Fan, G. (2024). Effect analysis of biomineralization for solidifying desert sands. *Biogeotechnics, 2*(1), https://doi.org/10.1016/j.bgtech.2023.100065

Naeem, M., Arab, M. G., Elbaz, Y., Omar, M., Ezzat, H., & Zeiada, W. (2024). Resilient behavior of bio-cemented sandy soil treated with enzyme-induced carbonate precipitation for pavement applications. *Construction Building Materials, 411*. https://doi.org/10.1016/j.conbuildmat.2023.134434

Pan, X., Chu, J., Yang, Y., & Cheng, L. (2020). A new biogrouting method for fine to coarse sand. *Acta Geotechnica, 15*(1), 1–16. https://doi.org/10.1007/s11440-019-00872-0

Shu, S., Yan, B., Ge, B., et al. (2022). Factors affecting soybean crude urease extraction and biocementation via enzyme-induced carbonate precipitation (EICP) for soil improvement. *Energies, 15*, 5566. https://doi.org/10.3390/en15155566

Šimůnek, J., Jarvis, N. J., Van Genuchten, M. T., & Gärdenäs, A. (2003). Review and comparison of models for describing non-equilibrium and preferential flow and transport in the vadose zone. *Journal of Hydrology, 272*(1-4), 14–35. https://doi.org/10.1016/S0022-1694(02)00252-4

Soto-Gómez, D., Juíz, L. V., Pérez-Rodríguez, P., et al. (2020). Percolation theory applied to soil tomography. *Geoderma, 357*, Article 113959. https://doi.org/10.1016/j.geoderma.2019.113959

Sun, X., Miao, L., & Wu, L. (2020). Applicability and theoretical calculation of enzymatic calcium carbonate precipitation for sand improvement. *Geomicrobiology, 37*(2), 1–11. https://doi.org/10.1080/01490451.2019.1710625

Sun, X., Miao, L., Chen, R., Wang, H., Wu, L., & Xia, J. (2021). Liquefaction resistance of biocemented loess soil. *Journal of Geotechnical and Geoenvironmental Engineering, 147*(11), Article 04021117. https://doi.org/10.1061/(ASCE)GT.1943-5606.0002638

Sun, F., Xiao, B., Li, S., et al. (2023). Direct evidence and mechanism for biocrusts-induced improvements in pore structure of dryland soil and the hydrological implications. *Journal of Hydrology, 623*, Article 129846. https://doi.org/10.1016/j.jhydrol.2023.129846

Thotakuri, G., Chakraborty, P., Singh, J., et al. (2024). X-ray computed tomography – Measured pore characteristics and hydro-physical properties of soil profile as influenced by long-term tillage and rotation systems. *Catena, 237*, Article 107801. https://doi.org/10.1016/j.catena.2023.107801

Wang, Y., Jiang, N., Saracho, A. C., Doygun, O., Du, Y., & Han, X. (2023b). Compressibility characteristics of bio-cemented calcareous sand treated through the bio-stimulation approach. *Journal of Rock Mechanics and Geotechnical Engineering,* (2), 510–522. https://doi.org/10.1016/j.jrmge.2022.05.007

Wang, H., Wang, J., Sun, X., Miao, L., Shi, W., Linyu, W. U., et al. (2023a). Erosion resistance of treated dust soils based on the combined enzymatically induced carbonate precipitation and polyacrylic acid. *Biogeotechnics, 1*(4), https://doi.org/10.1016/j.bgtech.2023.100050

Whiffin, V. S., Van Paassen, L. A., & Harkes, M. P. (2007). Microbial carbonate precipitation as a soil improvement technique. *Geomicrobiology Journal, 24*(5), 417–423. https://doi.org/10.1080/01490450701436505

Xu, K., Huang, M., Liu, Z., Cui, M., & Li, S. (2023). Mechanical properties and disintegration behavior of eicp-reinforced sea sand subjected to drying-wetting cycles. *Biogeotechnics, 1*(2), https://doi.org/10.1016/j.bgtech.2023.100019

Xu, P., Qian, H., Zhang, Q., & Zheng, L. (2021). Exploring the saturated permeability of remolded loess under inorganic salt solution seepage. *Engineering Geology, 294*, Article 106354. https://doi.org/10.1016/j.enggeo.2021.106354

Xu, P., Zhang, Q., Qian, H., Qu, W., & Li, M. (2020). Microstructure and permeability evolution of remolded loess with different dry densities under saturated seepage. *Engineering Geology, 282*(7), Article 105875. https://doi.org/10.1016/j.enggeo.2020.105875

Yang, X., Yan, M., & Zheng, J. (2024). Acid corrosion micro-macro mechanism of enzyme-induced carbonate precipitation (EICP) treated sandy soils. *Journal of Central South University, 31*, 636–648. https://doi.org/10.1007/s11771-024-5585-8

Zachara, J., Brantley, S., Chorover, J., Ewing, R., & Stack, A. G. (2016). Internal domains of natural porous media revealed: Critical locations for transport, storage, and chemical reaction. *Environmental Science Technology, 50*(6), 2811. https://doi.org/10.1021/acs.est.5b05015

Zhang, J., Xu, Z., Li, F., et al. (2017). Quantification of 3D macropore networks in forest soils in Touzhai valley (Yunnan, China) using X-ray computed tomography and image analysis. *Journal of Mountain Science, 14*, 474–491. https://doi.org/10.1007/s11629-016-4150-9

Zhang, Q., Ye, W., Liu, Z. R., Wang, Q., & Chen, Y. G. (2022). Influence of injection methods on calcareous sand cementation by eicp technique. *SSRN Electronic Journal*. https://doi.org/10.1016/j.conbuildmat.2022.129724

Zhang, M., Zhu, X., Yu, G., Yan, J., Wang, X., Chen, M., et al. (2015). Permeability of muddy clay and settlement simulation. *Ocean Engineering, 104*(aug.1), 521–529. https://doi.org/10.1016/j.oceaneng.2015.05.031